International Journal of
INTELLIGENT SYSTEMS AND APPLICATIONS IN ENGINEERING
ISSN:2147-6799 www.ijisae.org Original Research Paper

Enhanced Data Preservation in Light Field Hyperspectral Images through Combined Sparse Discrete Wavelet and PRN

P. Anjaneya[1], G. K. Rajini *[2]

Submitted: 25/09/2023 **Revised**: 16/11/2023 **Accepted**: 28/11/2023

Abstract: Lossless compression is a critical technique for reducing the storage and transmission requirements of light field hyper-spectral images, which are high-dimensional and data-intensive. The proposed approach Sparse Wavelet Decomposition and PRN for Lossless Compression (SDWT-PRN) leverages the advantages of both Sparse Discrete Wavelets Transform (SDWT) and Poincare recurrence neural network (PRN) for efficient and effective compression of light field hyper-spectral images. The SDWT is applied to decompose the light field hyper-spectral images into wavelet coefficients, which capture the multi-resolution and multi-directional information in the images. The PRRN is then employed to exploit the temporal redundancy among the wavelet coefficients to further compress the data. The proposed approach is evaluated on light field hyper-spectral image datasets, and the results demonstrate its superior compression performance compared to existing approaches. The investigational outcomes display that the combined SDWT and PRRN approach achieves high compression ratios while maintaining lossless reconstruction, making it suitable for efficient storage and transmission of light field hyper-spectral images in various applications, such as remote sensing, medical imaging, and scientific data analysis.

Keywords: *Hyperspectral, lossless compression, Sparse discrete wavelet transform, Poincare recurrence neural network.*

1. Introduction

Light field hyperspectral imaging is becoming increasingly popular in scientific research. Light field hyperspectral imaging captures both spatial as well as spectral data resulting in large amounts of data. Hyperspectral imaging is a powerful image acquisition technique that captures high-resolution spectral information across a wide range of wavelengths, enabling detailed analysis and interpretation of complex scenes [1-2]. In some applications, such as hyperspectral imaging pattern recognition [3-6], a succession of hyperspectral images taken across a single spatial area at different periods is required. However, hyperspectral data is often plagued by various types of noise, which can degrade the quality and accuracy of the data analysis. Additionally, hyperspectral data is inherently high-dimensional, resulting in challenges in storage and transmission. Therefore, efficient and effective pre-processing, dimensionality reduction, and lossless compression procedures are crucial for handling the acquired hyperspectral images.

The massive volumes of data that must be transmitted and stored limit the transmission and storage of hyperspectral images [7]. One of the most essential strategies for resolving such disagreements is data compression, which enhances transmission efficiency. The phrase nearly lossless, coined by some of the authors in 2000 [8], denotes that the distortion caused by compression has no effect on the outcomes of manual or automatic analysis done on compressed data. Hyperspectral images are large and contain vast amounts of data, which can make their storage and transmission challenging. Lossless compression techniques aim to compress the hyperspectral data without any loss of information, ensuring that the original data can be accurately reconstructed upon decompression. Various lossless compression methods have been proposed for hyperspectral data, including statistical-based methods, transform-based methods, and predictive methods. These methods exploit the inherent redundancy and regularity present in hyperspectral data to achieve compression without any loss of information.

The paper makes an important contribution to the field of image processing and data compression by developing a comprehensive algorithm. This paper presents an efficient dimensionality reduction technique based on the Discrete Wavelet Transform (DWT) and adaptive Thresholding based on the Birge-Massort strategy, which improves the algorithm's adaptability to image characteristics and noise levels. In addition, the use of the Poincare Recurrence Network (PRN) for hyperspectral data analysis provides a novel approach to recognizing recurring patterns and spectral clusters, providing valuable insights into data relationships. Furthermore, by including encryption and decryption procedures, the algorithm prioritizes data security. With image resizing and binarization capabilities, the workflow is not only innovative but also adaptable to a variety of image processing applications. This work advances the field as a whole by offering a comprehensive

[1] *School of Electronics Engineering, Vellore Institute of Technology, Vellore, Tamilnadu, India*
[2] *Professor, School of Electrical Engineering, Vellore Institute of Technology, Vellore, Tamilnadu, India*
** Corresponding Author Email: rajini.gk@vit.ac.in*

solution that streamlines various image processing tasks while also addressing dimensionality reduction, compression, and data security.

The paper is organized in a way that allows for a clear and logical progression of ideas. It starts with an introduction that describes the research problem and the paper's objectives. Following the introduction, a comprehensive review of relevant literature in the field establishes the context for the proposed system. The paper then expands on the proposed system, detailing the algorithm for image processing and data compression. This section describes the algorithm's steps, such as dimensionality reduction, thresholding, Poincaré Recurrence Network (PRN) analysis, and data security measures. The use of the Discrete Wavelet Transform (DWT), the Birge-Massort strategy, and other features such as image resizing and binarization are also discussed.

The paper then presents the results of applying the algorithm to real-world or simulated data after presenting the proposed system. The findings are accompanied by a detailed analysis that assesses the effectiveness of dimensionality reduction, the adaptability of Thresholding techniques, and the insights gained through PRN analysis.

The paper concludes with a summary of the main findings and contributions, discussion of their practical implications, addressing research limitations, and suggesting potential directions for future research in the field. The paper concludes with a reference list that cites all of the sources and references used throughout the paper.

2. Literature Review.

Light field hyperspectral images contain both spatial and spectral information, making them high-dimensional data. The storage and transmission of these images require large amounts of resources. Lossless compression is a technique that compresses data without losing any information.

Before moving into the survey of Compression procedures a brief overview of the basic image acquisition of Light Field Hyperspectral Imaging methods is provided in this paragraph. Starting with modern-day HSI acquisition, Duarte et al. (2008) and Ma et al. (2009) developed a single-pixel modality type of Imaging technology [9-10]. It is considered as an advanced technique in the hyperspectral image acquisition that enables the recovery of high-dimensional spectral information from a scene using a single detector element, or pixel, rather than an array of detectors as in traditional hyperspectral imaging systems. This approach has acknowledged as a best approach these days because it offers the potential to reduce the complexity and cost of hyperspectral imaging systems while maintaining high spectral resolution. In polarimetric spectrum imaging, Soldevila et al. (2013) suggested a new concept known as single-pixel optical system [11]. Wagadarikar et al. (2008) suggested a compressive sensing-based coded aperture snapshot spectral imaging System also referred as CASSI in brief form [12]. CASSI is a technique that uses a coded aperture to capture a snapshot of a scene's spectral content. The coded aperture is a patterned mask that is placed in front of a sensor, such as a camera, and is designed to modulate the incoming light in a way that encodes spectral information. By capturing multiple snapshots with different coded apertures, it is possible to reconstruct a hyperspectral image.

In recent years, various researchers have explored lossless compression of Light field hyperspectral images and thus we will discuss some of the recent methods proposed for lossless compression. Karami et al.(2010) suggested a 3D-DCT, a modified Discrete Cosine Transform fed on HIS [13]. The advantages of this work include efficiency, ease of implementation, and ability to retain important information, while its disadvantages include limited compression ratio, lossy compression, and sensitivity to image quality and more than that Parameters have to be manually selected.

Töreyn et al. (2015) projected an improved version of Joint photographic experts group-lossless [14]. Its advantages include high compression ratios, fast encoding and decoding speeds, and low computational complexity, while its limitations include high memory requirement, limited compression performance, sensitivity to noise, and lack of scalability. In this work overall CR depends heavily on the data.

Xu et al. (2017) suggested an approach that separated the input HSI into blocks, each with its own appropriate bit rate [15]. In this work the main focus was on the Multiple Linear regression which can be used in image compression for various tasks such as predictive coding, quantization, compression parameter optimization, rate-distortion optimization, and image quality assessment. It can help in modeling the relationship between different variables in the compression process, leading to improved compression performance and optimized results. Here Rate distortion not optimal and is a Lossy type of Compression.

Nascimento et. al (2018) proposed Compressive Sensing (CS) procedures [16]. Their advantages include high compression ratios, low computational complexity, robustness to noise and artifacts, and no need for prior knowledge. Their limitations include limited applicability, complex optimization, trade-off between compression ratio and reconstruction quality, and sensitivity to measurement errors.

Haut et. al (2019) suggested that Deep neural networks with autoencoders [17]. In summary, while deep neural networks, including autoencoders, have shown promise in

nonlinear compression of hyperspectral images, they also have limitations related to their complexity, computational cost, data requirements, potential for overfitting, interpretability and explainability, trade-offs between compression ratio and image quality, and robustness to noise and variability.

Deng et. al (2020) proposed a Generative Neural Network (GNN) is utilized for the purpose of image compression in Lossless mode [18]. Their advantages include high compression ratios, adaptive compression, low distortion, robustness to noise and artifacts, and fast compression and decompression. Their limitations include data requirements, high computational requirements, overfitting, and limited interpretability.

To address the snapshot compressive imaging (SCI) reconstruction problem, Meng et al. (2021) recommended employing untrained neural networks [8]. However, untrained neural networks may have some limited utility for hyperspectral image compression, their limitations make them less suitable than trained neural networks or other compression techniques.

Lee et al. (2022) suggested an image compression extended version of a sparse orthonormal transform [9] has shown promise in compression of hyperspectral images, it also has limitations related to computational complexity, dictionary design and training data, trade-off between sparsity and accuracy, sensitivity to noise and variability, interpretability and explainability, and scalability.

After a Comprehensive survey on related works of Hyperspectral Image Lossless Compression the observations and Limitations are presented in Table 1.

Table 1 Limitations of Image Compression Methods Reviewed.

S. No	**Mechanism Used with Reference Cited**	**Year of Publication**	**Observations**	**Limitations**
1	3D-DCT [13]	2010	ease of implementation, and ability to retain important information	limited compression ratio, lossy compression, and sensitivity to image quality
2	Joint photographic experts group-lossless [14]	2015	Spectral bands are subjected to a 1-D DWT	In this work overall CR depends heavily on the data.
3	Multiple linear regression [15]	2017	Partitioned the incoming HSI, giving each segment an appropriate BR.	Rate distortion not optimal and is a Lossy type of Compression.
4	Compressive Sensing (CS) techniques [16]	2018	advantages include high compression ratios, low computational complexity	limited applicability, complex optimization
5	Deep neural networks in the form of auto encoders [17]	2019	Cloud computing is used to implement the algorithm.	potential for over fitting
6	Generative Neural Network (GNN) [18]	2020	combined spectral/spatial correlation analysis	high computational requirements
7	untrained neural networks [19]	2021	uses a two-dimensional (2D) detector	less suitable than trained neural networks
8	Extended version of a sparse orthonormal transform [20]	2022	It is based on unions of orthonormal dictionaries	trade-off between sparsity and accuracy

3. Proposed System.

The proposed method as shown in Fig. 1 involves a combination of pre-processing for noise removal, Sparse discrete wavelet transforms (DWT) for dimensionality reduction, and Poincare recurrence neural network (RNN) for compression and decompression of hyperspectral data. This approach offers a comprehensive solution for efficient compression of large volumes of hyperspectral data, with minimal loss of information.

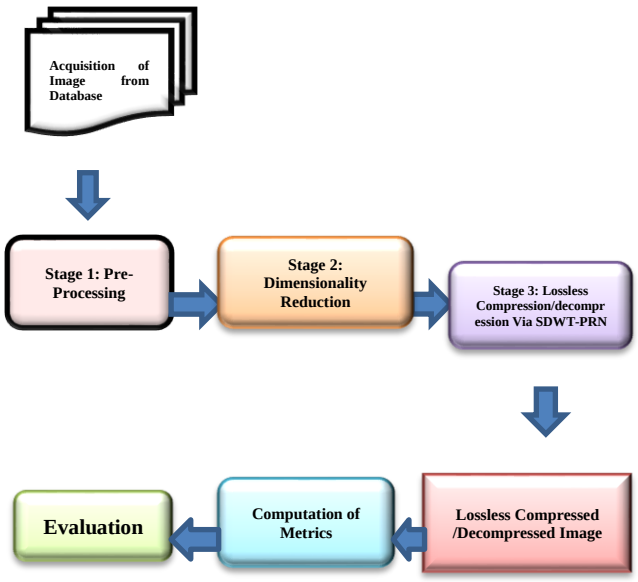

Fig. 1 Proposed Block diagrams.

The stepwise algorithms for the three stages of the proposed work with their internal mechanisms are provided in detail below.

Acquisition of Image form Hyperspectral Image database. Data augmentation is a method used to intentionally improve the diversity of the training data, and one method is the addition of noise using Gaussian functions. If the original image is denoted by I(x, y) where (x, y) denotes the corresponding pixel coordinates, and the Gaussian noise is denoted by N(x, y), the resulting noisy image can be obtained by adding the noise to the original image.

Noisy image = I(x, y) + N(x, y) …… (1)

Where N(x, y) denotes the Gaussian noise, which is generated based on a Gaussian distribution function with a mean value (denoted by μ) and its corresponding value of standard deviation (denoted by σ).

The formula for generating Gaussian noise is specified by:

N(x,y) = μ + σ * Z ……(2)

Where

• Z is considered as a random value attained from a standard Gaussian distribution, which has a mean value of 0 and the corresponding standard deviation value of 1.

• μ represents the mean of the Gaussian distribution, which determines the amount of shift in intensity, and

• σ represents the standard deviation of the Gaussian distribution, which determines the strength or amplitude of the noise.

Additionally, the image might be blurred due to various factors like motion or defocusing. So, image deblurring by means of Wiener Filter is carried out in order to reduce the noise. The Wiener Filter is a frequency-domain image restoration filter. It seeks to reduce the mean square error between the restored and original images. It takes into account both blurring degradation and additive noise.

Blurred Image = B(x,y) * I(x,y) + N(x,y)……(3)

Where: B(x, y) represents the blurring kernel, describing how the original image is convolved or blurred.

The objective is to restore the original, noise-free image I(x, y) from the noisy and blurred image. The Wiener Filter is used for this purpose. The Wiener Filter is defined as follows:

Restored Image = H*(f)/[H*(f)*H(f)+S(f)]*Noisy Image(f)….(4)

Where: **H (f)** represents the Fourier Transform of the blurring kernel B(x, y). **H*(f)** represents the complex conjugate of H (f). **S (f)** represents the power spectral density of the noise, which can be estimated from the noisy image. **Noisy Image (f)** represents the Fourier Transform of the noisy image. The division and multiplication are done element-wise in the frequency domain.

First, we normalize the restored image to have values within a certain range (for example, [0, 1]). This is typically accomplished by subtracting the image's minimum pixel value and then dividing by the range of pixel values.

Normalized Image(x,y) = (Restored Image(x,y)-Min)/(Max - Min)…..(5)

Where: Restored Image(x, y) is the pixel value in the restored image.

- **Min** is the minimum pixel value in the entire image.
- **Max** is the maximum pixel value in the entire image.

We perform contrast stretching after normalization to improve the image's contrast. This is accomplished by performing a linear transformation on the pixel values.

X=Enhanced Image(x,y) = Stretch Factor * Normalized Image(x,y) + Offset.....(6)

Where:

- Stretch Factor is a positive scaling factor.
- Offset is an optional offset value.

The stretch factor is determined by the desired level of contrast enhancement. One popular approach is to specify two limits, the lower limit (LL) and the upper limit (UL), and calculate the stretch factor as follows:

Stretch Factor = (UL - LL)…….. (7)

The offset parameter is employed to displace the pixel values. The adjustment is discretionary and has the potential to be adjusted to a value of zero in order to implement standard contrast stretching. In the event that an offset is

employed, it results in a displacement of the complete range of intensities.

Offset = LL……(8)

Now we move towards the dimensionality reduction stage. Declaration of Variables such as coefficient of scaling, lifting steps and layer type transformation. Sub sampling based on lifting steps that have been declared. Compute the Transformation function by means of Discrete Wavelet transform.

The transformation function can be mathematically represented as follows:

T(C)=f(C)…… ……(9)

Where T(C) represents the transformation function applied to the coefficients C obtained from the DWT, and f(C) represents the specific processing applied to the enhancement from the previous stage. Carry out the retrieval process of detail coefficients. Apply Boundary Conditions for tracing purpose and Initiate Inverse Transform. Attain the Dimensionality reduced outcome in form a resultant image. Now the next step is to carry out Lossless Compression as well as decompression Via Poincare. The resultant image from the previous stage is subjected here as input

Initiate 2-D Wavelet decomposition via 'dmey' . Let X be enhanced version of the image, and W be the 2D wavelet transform of X using a specific wavelet function. The 2D wavelet decomposition can be mathematically expressed as:

$$W\_j,k = \sum (h\_i,j * X\_k-i,l-j) \text{ for } 0 \leq i < N, 0 \leq j < M \quad \ldots\ldots(10)$$

Where:

- W_j,k is the coefficient of the wavelet transform at the j-th scale and k-th position
- h_i,j is the wavelet filter coefficient at the i-th scale and j-th position
- X_k-i,l-j is the pixel value of the input image at the k-i-th row and l-j-th column
- N and M are the dimensions of the wavelet filter

The formula represents a convolution operation between the wavelet filter coefficients (h_i,j) and the input image (X) at different scales and positions, followed by a summation to obtain the wavelet coefficients (W_j,k).

Declaration of threshold for Wavelet 2D using Birge-Massort strategy which involves estimating the threshold value. Within the framework of wavelet-based Thresholding, the Birge-Massort strategy entails the estimation of a threshold value for the purpose of discerning which wavelet coefficients should be retained and which should be discarded.

The estimation of the threshold value (T) can be performed using the Birge-Massort strategy. The estimation of the threshold is commonly derived from the statistical characteristics of the wavelet coefficients. The determination of the threshold value typically relies on the noise level (σ) present in the image.

T = Threshold Estimation Function (σ)…….. (11)

Analyze the compressed hyperspectral data using the Poincare Recurrence Network (PRN). This step entails, creating a Poincare section that selects specific hyperspectral regions and recognizing recurring states in compressed data.

Building a network based on recurrence patterns, with nodes representing states and edges representing recurrent connections. Analyze the PRN for hyperspectral data to learn more about the dynamics and spatial-spectral relationships. Recognize recurring patterns or spectral clusters. Network properties such as connectivity and centrality are measured. PRN features are extracted for further processing of Compression process.

Compression process based on real valued matrix and that too via Hard Thresholding and obtaining the Compressed Image. In the context of wavelet-based image compression and also involving PRN here, we employ hard Thresholding as a means to eliminate coefficients that possess values below a specified threshold. The representation of the thresholded wavelet coefficients can be expressed in the following manner.

Compressed Coefficients (W_j,k_compressed) =

W_j,k if |W_j,k| > T,0 otherwise……(12)

The compressed image is derived through the application of the inverse two-dimensional wavelet transform on the compressed coefficients.

Compressed Image (X_compressed) = Inverse 2D Wavelet Transform W_j,k_compressed)……..(13)

The act of adjusting the dimensions of an image to a predetermined number of rows (R) and columns (C) is a frequently performed task. The resizing operation is executed by employing interpolation techniques, specifically bilinear interpolation.

Resized Image (X_resized) = Interpolation (X_compressed,R,C)……(14)

The process of binarization is commonly executed by applying a threshold to the grayscale image, resulting in the generation of a binary image. The thresholding operation can be mathematically represented as:

Binary Image (X_binary) = Binarization (X_resized,Threshold)…….(15)

Encryption and Decryption procedures are carried out to

attain the Lossless de-compressed image. Within the realm of image compression and decompression, encryption and decryption techniques are employed to safeguard the integrity and confidentiality of the image data. One prevalent method of encryption entails the utilization of a cryptographic algorithm to manipulate the data within an image.

$$\text{Encrypted\_Image} = \text{Encryption\_Algorithm}(X\_binary, Key) \quad \text{.....(16)}$$

$$\text{Decrypted\_Image} = \text{Decryption\_Algorithm}(\text{Encrypted\_Image}, Key) \quad \text{.....(17)}$$

The mathematical expression for deriving the decompressed image subsequent to decryption can be formulated as follows:

$$\text{Decompressed Image } (X\_decompressed) = \text{Decryption\_Algorithm } (\text{Encrypted\_Image}, Key) \quad \text{.....(18)}$$

3.1 Proposed Model:

The described process in model as shown in Fig. 2 is a comprehensive pipeline that combines advanced signal processing, image compression, and data security techniques. Its multifaceted approach demonstrates its novelty and justification. The title "Sparse Wavelet Decomposition and PRN for Lossless Compression - SWaPR-Net" justifies the methodology's core components in a clear and concise manner. It starts off by emphasizing the use of Sparse Wavelet Decomposition (SWD), which stands for selective data representation and redundancy reduction. Furthermore, the title introduces the novel inclusion of the Poincare Recurrence Network (PRN) for lossless compression, which is a distinguishing feature of this approach. This combination is conveniently encapsulated by the acronym SWaPR-Net, emphasizing the interconnected nature of the two reference techniques.

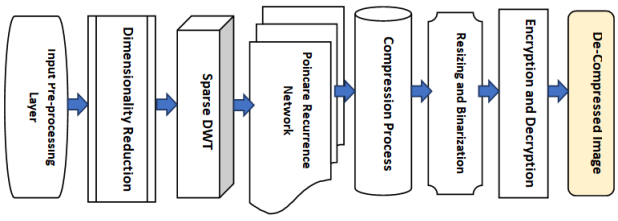

Fig.2 Proposed Model architecture

The combination of Sparse Wavelet Decomposition (SWD) and Poincare Recurrence Network (PRN) for lossless compression is what makes this methodology unique. When combined with PRN, SWD's selective data representation effectively reduces redundancy, introducing a novel application in lossless compression. PRN is not commonly associated with data compression because it is typically used for analyzing complex dynamic systems. The combination of these two techniques provides a novel approach, and the provided SWaPR-Net acronym emphasizes the innovation in combining these data compression methodologies.

3.2 Algorithm of proposed model

The proposed model in a stepwise manner is provided in the following algorithm. This algorithm is intended to process and compress images, making it suitable for image storage, transmission, and secure data transfer applications. To ensure efficient compression while maintaining data security, it combines dimensionality reduction, wavelet-based compression, and data encryption. Because it includes image resizing and binarization, it is adaptable to a variety of image processing tasks.

Algorithm : Proposed Algorithm

Step 1: Dimensionality Reduction
// Declare Coefficient of Scaling, Lifting Steps, Layer Type Transformation
// Apply Sub sampling based on Lifting Steps.
// Compute Transformation Function using DWT
// T(C) = f(C) where T(C) represents the transformation and f(C) specific processing
// Retrieve Detail Coefficients
// Apply Boundary Conditions
// Initiate Inverse Transform
// Resultant Image is the outcome
Step 2: Lossless Compression
// Use Resultant Image as Input
// Initiate 2-D Wavelet Decomposition with 'dmey' wavelet
// Let X be the enhanced image, and W be the 2D wavelet transform of X
// Apply 2D Wavelet Decomposition: $W\_j,k = \sum (h\_i,j * X\_k-i,l-j)$
// Declare Threshold for 2D Wavelet using Birge-Massort Strategy
// Estimate Threshold (T) based on noise level (σ) in the image
// Apply Hard Thresholding: $W\_j,k\_compressed = W\_j,k$ if $|W\_j,k| > T$, 0 otherwise
// Compressed Image is derived through Inverse 2D Wavelet Transform
Step 3: Image Resizing
// Adjust Compressed Image to R rows and C columns
// Resize using Bilinear Interpolation
// Resized Image is the output
Step 4: Binarization

// Apply Threshold to Resized Image to generate Binary Image

Step 5: Encryption and Decryption

// Encrypt Binary Image with Encryption Algorithm and Key.

// Decrypted Image is derived by applying Decryption Algorithm with the Key

Step 6: Decompressed Image

// The Decompressed Image is obtained as the final output After Decryption.

4. Results and Analysis.

For the purpose of Investigation, the sample image as shown in Fig.3 from the dataset of Hyperspectral Images is considered.

Fig. 3 Original Image

Fig. 4 Resized Image

In Pre-processing stage, the original Image from the samples of database is resized as shown Fig. 4 before adding Gaussian Noise and later Wiener filter is used to remove the noise and its resultant is shown in Fig. 5. The image is further contrast enhanced to improve the quality of the Noise removed image as revealed in Fig.6.

Fig. 5 Noise Removed Image

Fig. 6 Quality Improved Image.

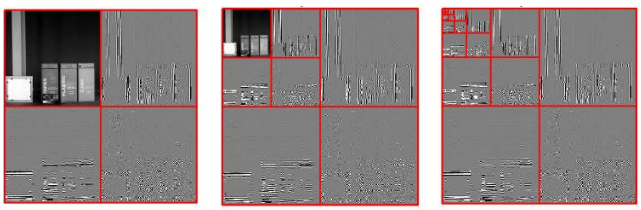

Fig. 7 (a), (b) &(c) SDWT Spatial Pre-Processing Stages of Image.

The quality improved image later subjected to second stage where at first SDWT Spatial Pre-processing is carried out to achieve the wavelet decomposed images as shown if Fig. 7 (a), 7 (b) & 7 (c). Further the image is reduced for its dimensionalities as shown in Fig. 8.

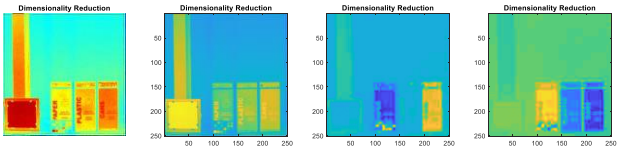

Fig. 8 Dimensionality Reduction Processed Images**.**

The dimensionality reduced image is subjected to third stage of Poincare RNN where the encryption and decryption procedures are carried out. Thus, the resultant lossless compressed image is shown in Fig. 9 after carrying out the proposed method.

Fig. 9 Lossless Compressed Image

The further investigation has been carried out for quality metrics such as Average Difference (AD), Normalized Cross-correlation (NC), Maximum Difference (MD) Structural Content (SC), and Normalized Absolute Error (NAE).

4.1 Quality Metrics.

A.Normalized Cross-Correlation (NCC).

The NCC is a metric for comparing two sets of images. In image processing presentations where the image's brightness can be vary due to lighting and also exposure circumstances, the images can first be normalized. It is used to determine the number of instances of a pattern or object in a picture. A frequently used parameter that aids in determining the gradation of similarity or dissimilarity among the reconstructed and original images. Normally, the NCC value ranges between -1 and 1. If the NCC value is'1 ', the image arrangement in the time series is precise, but amplitude will be vary and is characterized in following equation.

$$NCC=\sum_{x=1}^{M}\sum_{y=1}^{N} I(x,y).I'(x,y) \quad \ldots\ldots\ldots\ldots\ldots\ldots (19)$$

B. Average Difference (AD).

The average difference is the difference in pixels between the filtered and degraded images. This quantitative degree is utilized exclusively in object detection and identification applications, but it can also be used in any image processing application where the average difference between two

images is determined as provided below.

Average Difference is defined as AD=Error/(MxN),

Error = (Original Image – Reconstructed Image)

$$AD = \frac{1}{MN}\sum_{x=1}^{M}\ \sum_{y=1}^{N}[I(x,y) - I'(x,y)] \ldots\ldots\ldots\ldots (20)$$

C. Structural Content (SC).

The structural content of an image is concerned with the spatial organization of its pixels. It determines the proximity of two digital images, which may alternatively be expressed as a correlation function. This metric is used to determine the degree of resemblance between two photographs. It eliminates the intimate relationship between two images and says that the human eye is incapable of distinguishing the two images. The degree of correspondence between images is determined by their structural contents and is presented below.

$$SC = \frac{\sum_{x=1}^{M}\ \sum_{y=1}^{N}[I(x,y)]^2}{\sum_{x=1}^{M}\ \sum_{y=1}^{N}[I'(x,y)]^2} \ldots\ldots\ldots\ldots (21)$$

D. Maximum Difference (MD).

It is proportional to contrast and so determines the dynamic range of a picture. It is accomplished by sending a picture through a low pass filter, as sharp edges correlate to the image's higher frequency parts, which the low pass filter suppresses. It illustrates a variation on the matching assessments method and represented in below equation.

$$MD=\text{Max}(|I(x,y) - I'(x,y)|) \ldots\ldots (22)$$

E. Normalized Absolute Error (NAE).

This is the standard measure, and it may be used to detect blurring in any real-time image. This calculates the arithmetical variance between the original image and the resultant image from the proposed work specified in equation below.

$$NAE=\frac{\sum_{x=1}^{M}\ \sum_{y=1}^{N}|I(x,y)-I'(x,y)|}{\sum_{x=1}^{M}\ \sum_{y=1}^{N}I(x,y)} \ldots\ldots\ldots\ldots (23)$$

Sample	Quality Metrics				
	NC	AD	SC	MD	NAE
Image 1	1.085	-16.2	0.84	13	0.109
Image 2	1.062	-8.23	0.92	16	0.025
Image 3	0.98	0.001	0.89	14	0.110
Image 4	1.078	-9.25	0.982	45	0.105
Image 5	1.065	-6.25	0.921	34	0.102

4.2 Performance assessment

Compression ratio simply refers to the ratio of the output to the input hyperspectral image size involved in compression/decompression. In other words, it is the ratio of original image size to the compressed bit stream size. It is mathematically expressed as given below.

$$CR = \frac{O_{IS}}{C_{IS}} \ldots\ldots\ldots\ldots (24)$$

With the equation (24), the compression ratio 'CR' is dignified constructed on the original image size 'O_{IS}' and the compressed image size 'C_{IS}'. Table 3 given below reports the compression ratio over the trial set realized by the numerous methods [21] and [22].

Table 3 Compression ratio of Proposed SDWT-PRN and Existing GDW-PRN[23], C-DPCM [21] and 3DWT-SRV [22]

Samples	Compression ratio (mb)			
	Proposed SDWT-PRN	GDW-PRN [23]	C-DPCM [21]	3DWT-SRV [22]
Image 1	**1.26**	1.54	1.76	1.976
Image 2	**1.84**	1.95	2.15	2.25
Image 3	**1.89**	2.05	2.3	2.45
Image 4	**1.95**	2.15	2.45	2.6
Image 5	**2.12**	2.28	2.55	2.9
Image 6	**2.21**	2.55	2.95	3.15
Image 7	**2.34**	2.95	3.15	3.85
Image 8	**2.89**	3.05	3.3	4.25
Image 9	**2.91**	3.15	3.55	4.45
Image 10	**3.05**	3.3	3.95	4.6

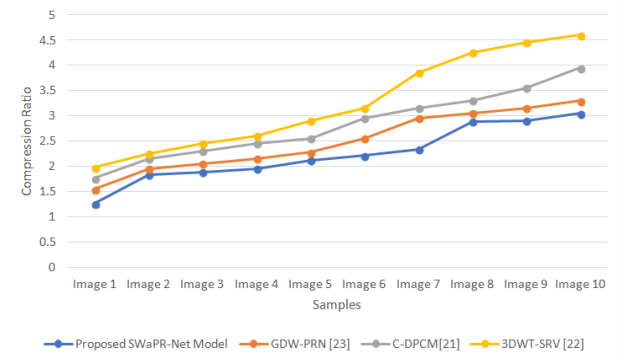

Fig 10 Graphical representation of compression ratio.

Above depicts the compression ratio evaluated for 10 different images of varying sizes. From figure 12 it is evident that the compression ratio is right proportionate to the samples provided. In other words, different samples result in different compression ratio. The proposed SDWT-

PRN Model has shown a commendable compression ratio for a sequence of hyperspectral images, outperforming previous works such as GDW-PRN [23], C-DPCM [21], and 3DWT-SRV [22]. This means that the SDWT-PRN Model outperforms these established methods in terms of hyperspectral data compression efficiency.

Table 4 compares Light Field Image Storage between the proposed SDWt-PRN model and previously published works, namely GDW-PRN [23], C-DPCM [21], and 3DWT-SRV [22]. This table demonstrates the SDWT-PRN model's efficiency in terms of storage requirements, emphasizing its superiority in minimizing storage demands for light field images.

Samples	Light field images storage (KB)			
	Proposed SDWT-PRN	GDW-PRN [23]	C-DPCM [21]	3DWT-SRV [22]
Image 1	**21**	**30**	**45**	**60**
Image 2	**42**	**60**	**90**	**120**
Image 3	**78**	**90**	**100**	**140**
Image 4	**101**	**120**	**135**	**160**
Image 5	**111**	**140**	**160**	**190**
Image 6	**131**	**180**	**190**	**210**
Image 7	**147**	**210**	**230**	**250**
Image 8	**163**	**230**	**280**	**310**
Image 9	**189**	**250**	**300**	**340**
Image 10	**210**	**290**	**340**	**390**

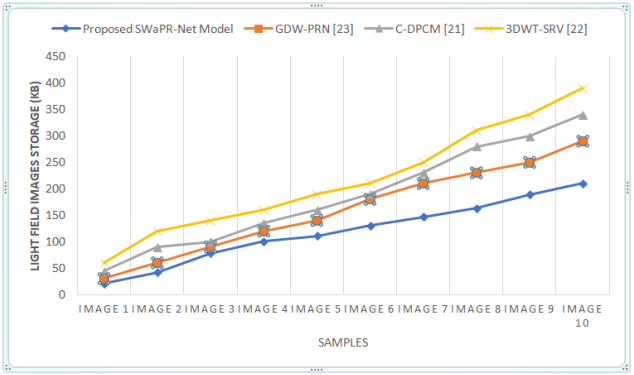

Fig 11 Graphical representation of storage (KB).

Above figure 11 presents a graphical depiction of the data, wherein the x-axis denotes distinct samples and the y-axis portrays the storage capacity of Light Field Images in kilobytes (KB). The graphical representation provides visual evidence that supports the conclusions outlined in Table 4, highlighting the superior performance of the SDWT-PRN model compared to GDW-PRN [23], C-DPCM [21], and 3DWT-SRV [22] in terms of storage efficiency.

Table 5 presents a comparative analysis of the Peak Signal-to-Noise Ratio (PSNR) values for the SDWT-PRN model and the aforementioned existing works, namely GDW-PRN [23], C-DPCM [21], and 3DWT-SRV [22]. The table presents a comparison of different methods, demonstrating that the SDWT-PRN model achieves superior peak signal-to-noise ratio (PSNR) outcomes in comparison to the alternative approaches. This finding underscores the model's capacity to minimize storage requirements while preserving a high level of image fidelity.

Table 5 PSNR values comparison

Samples	PSNR (dB)			
	Proposed SDWT-PRN	GDW-PRN [23]	C-DPCM [21]	3DWT-SRV [22]
Image 1	48.23	39.04	37.3	35.85
Image 2	49.32	41.35	38.35	36.15
Image 3	48.43	42.55	39.55	37
Image 4	49.88	43.15	40.15	38.35
Image 5	50.23	45.55	41.35	39.01
Image 6	51.11	46	42	40.25
Image 7	51.45	46.15	44.55	40.35
Image 8	52.12	46.85	45.35	41.2
Image 9	52.76	47	45.85	42.45
Image 10	52.89	47.35	46.25	43.21

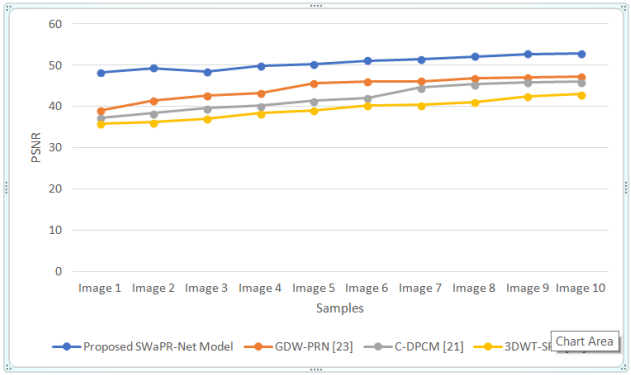

Fig 12 Graphical representation of PSNR

The visual representation in Figure 12 illustrates the PSNR values, where the x-axis represents various samples and the y-axis represents the corresponding PSNR values. The graphical representation supports the results presented in

Table 5, highlighting the consistent ability of the SDWT-PRN model to produce higher Peak Signal-to-Noise Ratio (PSNR) values in comparison to GDW-PRN [23], C-DPCM [21], and 3DWT-SRV [22]. The visual representation serves to enhance the perception of the model's exceptional image quality.

5. Conclusion

In this article, a combined method for lossless hyperspectral image compression and decompression is presented that incorporates pre-processing for noise removal, Sparse Discrete Wavelet Transforms (SDWT) for dimensionality reduction, and Poincare recurrence neural network (PRNN) for lossless compression and decompression. The different quality metrics to examine the suggested method, including Average Difference (AD), Normalized Cross-correlation (NC), Maximum Difference (MD), Structural Content (SC), and Normalized Absolute Error (NAE) (NAE) were utilized. For 10 different hyperspectral images, our experimental results show that the suggested method produces improved compression ratios and surpasses the existing methods published in the literature. The proposed method will be extended in the future to include lossy compression techniques in order to obtain even greater compression ratios along with optimal PSNR and image storage capacity. We also intend to investigate the applicability of our method to various types of hyperspectral images collected by different sensors and under varied conditions. Another possible direction for future research is to use our technology to compressing hyperspectral videos.

Author Contributions

P. Anjaneya: Conceptualization, Data curation Formal analysis, Methodology, Software Writing, original draft, investigation, resources.

G.K. Rajini: Writing—review and editing, visualization, supervision, project administration.

Conflicts of Interest

The authors declare that they have no known competing financial interests or personal relationships that could have appeared to influence the work reported in this paper.

References:

[1] Goetz, A.F., (2009). Three decades of hyperspectral remote sensing of the Earth: A personal view. Remote Sensing of Environment, 113, pp.S5-S16.

[2] Eismann, M.T., (2012), April. Hyperspectral remote sensing. Bellingham: SPIE.

[3] Thouvenin, P.A.; Dobigeon, N.; Tourneret, J.Y. A Hierarchical Bayesian Model Accounting for Endmember Variability and Abrupt Spectral Changes to Unmix Multitemporal Hyperspectral Images. IEEE Trans. Comput. Imag. 2018, 4, 32–45. [CrossRef]

[4] Marinelli, D.; Bovolo, F.; Bruzzone, L. A novel change detection method for multitemporal hyperspectral images based on a discrete representation of the change information. In Proceedings of the 2017 IEEE International Geoscience and Remote Sensing Symposium (IGARSS), Fort Worth, TX, USA, 23–28 July 2017; pp. 161–164.

[5] Liu, S.; Bruzzone, L.; Bovolo, F.; Du, P. Unsupervised Multitemporal Spectral Unmixing for Detecting Multiple Changes in Hyperspectral Images. IEEE Trans. Geosci. Remote Sens. 2016, 54, 2733–2748.

[6] Ertürk, A.; Iordache, M.D.; Plaza, A. Sparse Unmixing-Based Change Detection for Multitemporal Hyperspectral Images. IEEE J. Sel. Top. Appl. Earth Obs. 2016, 9, 708–719

[7] R. B. Gomez, "Hyperspectral imaging: a useful technology for transportation analysis," Opt. Eng. 41(09), 2137- 2143 (2002).

[8] B. Aiazzi, L. Alparone, and S. Baronti, “Information preserving storage of remote sensing data: virtually lossless compression of optical and SAR images,” in Proceedings of the International Geoscience and Remote Sensing Symposium (IGARSS ’00), pp. 2657–2659, July 2000.

[9] M. F. Duarte, M. A. Davenport, D. Takhar, and J. N. Laska, “Single-pixel imaging via compressive sampling,” IEEE Signal Process. Mag. 25(2), 83-91 (2008).

[10] J. Ma, “Single-pixel remote sensing,” IEEE Geosci. Remote Sens. Lett. 6(2), 199- 203(2009).

[11] F. Soldevila, E. Irles, V. Durán, P. Clemente, M. Fernández-Alonso, E. Tajahuerce, et al., "Single-pixel polarimetric imaging spectrometer by compressive sensing," Applied Physics B, 113, 551-558(2013).

[12] A. Wagadarikar, N. P. Pitsianis, X. Sun, and D. J. Brady, "Spectral image estimation for coded aperture snapshot spectral imagers," Proc. SPIE, 7076, 707602–707602–15 (2008).

[13] Karami, M. Yazdi, and A. Z. Asli, “Hyperspectral image compression based on tucker decomposition and discrete cosine transform,” in 2nd Int. Conf. Image Process. Theory, Tools and Appl., IEEE, pp. 122–125 (2010).

[14] U. Töreyn et al., “Lossless hyperspectral image compression using wavelet transform based spectral decorrelation,” in 7th Int. Conf. Recent Adv. Space Technol., IEEE, pp. 251–254 (2015).

[15] K. Xu et al., “Distributed lossy compression for hyperspectral images based on multilevel coset codes,” Int. J. Wavelets Multiresolution Inf. Process. 15(2), 1750012 (2017).

[16] Nascimento, J.M.P.; V’Estias, M.; Duarte, R. Hyperspectral compressive sensing: A low-power consumption approach. Int. Soc. Opt. Eng. 2018, 10792, 1079202

[17] Haut, J.M.; Gallardo, J.A.; Paoletti, M.E.; Cavallaro, G.; Plaza, J.; Plaza, A.; Riedel, M. Cloud Deep Networks for Hyperspectral Image Analysis. IEEE Trans. Geosci. Remote Sens. 2019, 57, 9832–9848.

[18] S. Rajkumar* and G. Malathi “A Comparative Analysis on Image Quality Assessment for Real Time Satellite Images” Int. J. Science and Technology, Vol 9(34), DOI: 10.17485/ijst/2016/v9 i34/96766, September 2021.

[19] Meng, Z., Yu, Z., Xu, K. and Yuan, X., Self-supervised neural networks for spectral snapshot compressive imaging. Proc. IEEE Int. Conf. Comput. Vis. 2602–2611 (2021)

[20] Gihwan Lee and Yoonsik Choe. Fast and efficient union of sparse orthonormal transforms via dct and bayesian optimization. Applied Sciences, 12(5):2421, 2022.

[21] Jiqiang Luo, Jiaji Wu, Shihui Zhao, Lei Wang, Tingfa Xu1, “Lossless compression for hyperspectral image using deep recurrent neural networks”, International Journal of Machine Learning and Cybernetics, Feb 2019 [Compression based on Differential Pulse Code Modulation (C-DPCM)]

[22] Nadia Zikiou, Mourad Lahdir, David Helbert, “Support vector regression-based 3D-wavelet texture learning for hyperspectral image compression”, The Visual Computer, Springer, Sep 2019 [3D Wavelet Transform and Spectrum learning with Regression Vector (3DWT-SRV)]

[23] Anjaneya P and Rajini G. K. "Light Field Hyper Spectral Lossless Compression Employing Greedy Discrete Wavelet and Poincare Recurrence Network." International Journal of Intelligent Engineering and Systems, vol. 16, no. 5, 2023, DOI: 10.22266/ijies2023.1031.33.